

# Hydride Transfer Reduction of Carbonyls by a Rhodium(I) Complex: A Theoretical Study. 1. The Two-Step Mechanism

Vincent Guiral, Françoise Delbecq, and Philippe Sautet\*

*Institut de Recherches sur la Catalyse, 2 Avenue Albert Einstein,  
69626 Villeurbanne Cedex, France, and Laboratoire de Chimie Théorique,  
Ecole Normale Supérieure, 46 Allée d'Italie, 69364 Lyon Cedex 07, France*

Received July 30, 1999

The two-step mechanism for the catalytic cycle of carbonyl reduction by a rhodium(I) hydride model complex,  $\text{RhH}(\text{NH}_3)_2(\text{C}_2\text{H}_4)_2$ , was studied on the basis of DFT theoretical calculations. This assumed mechanism consists of the dissociation of a N–Rh bond on the hydride complex, the coordination of the carbonyl, followed by the hydride migration, the recoordination of the N-ligand, and finally the exchange of alkoxy ligands to give the desired alcohol. The cycle is terminated by the reverse reactions, acetone is eliminated, and the hydride complex is regenerated. Several substrates such as formaldehyde, acetone, and the experimentally used acetophenone were investigated as starting materials. Each postulated intermediate was confirmed to be a stationary point on the potential energy surface, and transition states were determined. The potential energy profile was found to be smooth without excessive activation barriers. The hydride migration and its reverse reaction ( $\beta$ -H transfer) are found to be the rate-determining steps.

## I. Introduction

Asymmetric reduction of C=O bonds by hydride transfer leading to optically active secondary alcohols is one of the major challenges in modern chemistry. It can be achieved by means of transition metal, such as Ru(II), Rh(I), and Ir(I), bearing chiral ligands. Besides phosphorus ligands, which have been extensively used,<sup>1</sup> nitrogen-containing ligands are now widely considered: they present many advantages (more accessible, cheaper, more stable), and previous studies<sup>2–5</sup> showed that they can be used in asymmetric reduction of carbonyls with similar or even higher selectivities than those obtained with the best chiral phosphines. For example, 67% ee at 100% conversion has been reported<sup>3</sup> for the hydride transfer reduction of acetophenone, in 2-propanol at room temperature, using *N,N*-dimethyl-1,2-diphenyl-1,2-ethanediamine and  $[\text{Rh}(\text{COD})\text{Cl}]_2$  as metallic precursor (Figure 1).

Although the results are satisfactory in terms of efficiency and selectivity, little is known experimentally

about intermediates and reaction steps, and the mechanism of the reaction has not yet been elucidated. Some mechanisms have been proposed for asymmetric hydrogen transfer reaction.<sup>6,7</sup> Two general paths could be envisaged:<sup>6,7</sup> a stepwise process through an intermediate hydride complex (path A) and a concerted process where the hydrogen is directly transferred from the secondary alkoxy complex to the coordinated substrate (path B). In the case of path A, two possibilities can be considered: a two-step mechanism with coordination of the substrate followed by an intramolecular hydride migration and a concerted one as proposed by Gladiali et al.<sup>5</sup> Up to now, only a kinetic study on this reaction has been performed.<sup>8</sup> Our purpose is to elucidate the mechanism of this reaction in the case of rhodium catalysts bearing chiral nitrogen, by means of DFT calculations, to find the origin of the enantioselectivity. Understanding the detailed mechanism of the reaction should allow us to obtain insights for improvement of the enantioselectivity.

In a previous work<sup>7</sup> we have investigated the structure of the supposed hydride intermediate complex. In the present paper we will present our results for one of the possible mechanisms, the two-step mechanism of path A. This path has been studied first because it has been often suggested for different systems. For example, it was proposed by Wilkinson et al.<sup>9</sup> in the case of the

\* Corresponding author. Tel: 00 33 4 72 44 53 48. Fax: 00 33 4 72 44 53 99. E-mail: sautet@catalyse.univ-lyon1.fr.

(1) (a) Spogliarich, R.; Kaspar, J.; Graziani, M.; Morandini, F.; Piccolo, O. *J. Catal.* **1985**, *94*, 292. (b) Spogliarich, R.; Kaspar, J.; Graziani, M.; Morandini, F.; Piccolo, O. *J. Organomet. Chem.* **1986**, *306*, 407.

(2) Hashigushi, S.; Fujii, A.; Takehara, J.; Ikariya, T.; Noyori, R. *J. Am. Chem. Soc.* **1995**, *117*, 7562.

(3) (a) Gamez, P.; Fache, F.; Mangeney, P.; Lemaire, M. *Tetrahedron Lett.* **1993**, *34*, 6897. (b) Gamez, P.; Fache, F.; Lemaire, M. *Tetrahedron: Asymmetry* **1995**, *6*, 705. (c) Gamez, P.; Dunjic, B.; Fache, F.; Lemaire, M. *Tetrahedron: Asymmetry* **1995**, *6*, 1109.

(4) (a) Fache, F.; Gamez, P.; Nour, F.; Lemaire, M. *J. Mol. Catal.* **1993**, *85*, 131. (b) Touchard, F.; Bernard, M.; Fache, F.; Delbecq, F.; Guiral, V.; Sautet, P.; Lemaire, M. *J. Organomet. Chem.* **1998**, *567*, 133.

(5) Gladiali, S.; Pinna, L.; Delogu, G.; De Martin, S.; Zassinovich, G.; Mestroni, G. *Tetrahedron: Asymmetry* **1990**, *1*, 635.

(6) Zassinovich, G.; Mestroni, G. *Chem. Rev. (Washington, D.C.)* **1992**, *92*, 1051.

(7) Bernard, M.; Guiral, V.; Delbecq, F.; Fache, F.; Sautet, P.; Lemaire, M. *J. Am. Chem. Soc.* **1998**, *120*, 1441.

(8) de Bellefon, C.; Tanchoux, N. *Tetrahedron: Asymmetry* **1998**, *9*, 3677.

(9) (a) Evans, D.; Osborn, J. A.; Wilkinson, G. *J. Chem. Soc. A* **1968**, 3133. (b) Evans, D.; Yagupsky, G. *J. Chem. Soc. A* **1968**, 2660. (c) Brown, C. K.; Wilkinson, G. *J. Chem. Soc. A* **1970**, 2753.

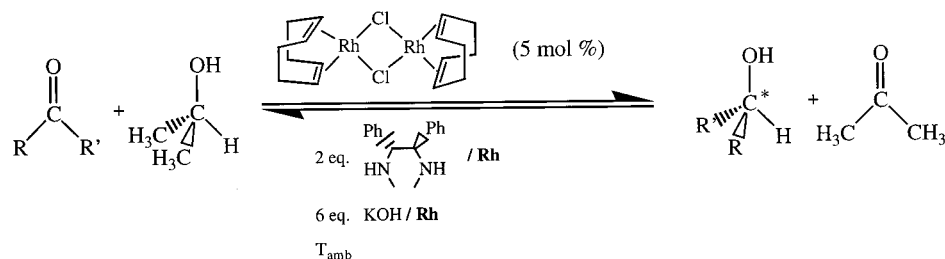


**Figure 1.** Asymmetric hydride transfer reduction of acetophenone.

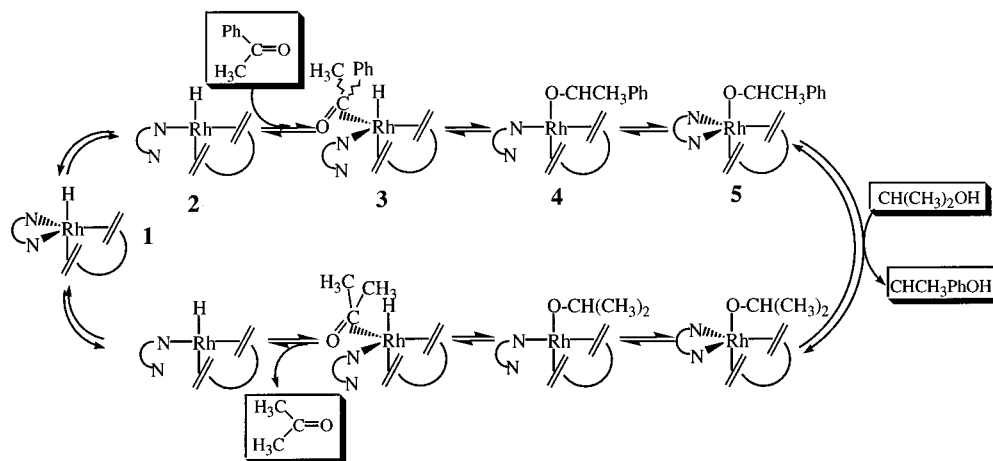


**Figure 2.** Proposed catalytic cycle for the reduction of acetophenone with Rh(I) hydride complex.

olefin hydroformylation catalyzed by  $\text{RhH}(\text{CO})_2(\text{PPh}_3)_2$ : in the first step, the departure of one of the two phosphine ligands takes place, followed by the coordination of the olefin ligand. Farnetti et al.<sup>10</sup> also assumed a similar mechanism for the reduction of carbonyl by hydrogen transfer catalyzed by Ir(I)/P–N systems: the amino group of the bidentate P–N ligand decoordinates reversibly prior to carbonyl coordination.

Figure 2 shows the various steps that we have considered in the case of hydride transfer between 2-propanol and acetophenone. This cycle starts with the postulated hydride complex **1**.<sup>7</sup> The first step involves the reversible dissociation of a N–Rh bond leading to the neutral  $\text{ML}_4$  16-electron complex **2**. Since the  $\text{ML}_4$  complex is an unsaturated one, it can add a carbonyl to form a  $\eta^1$  or  $\eta^2$   $\text{ML}_5$  complex **3**. The hydride can move to the carbon of the coordinated carbonyl to give the  $\text{ML}_4$  alkoxy complex **4**, which leads to **5** after recoordination of the N-ligand. Then, there is an exchange with the 2-propanol solvent followed by the reverse reactions (dissociation of nitrogen-containing ligand,  $\beta$ -H transfer, carbonyl elimination, and recoordination of N-ligand), leading to the regeneration of **1**.

In the present theoretical study, we focused on the first steps (from **1** to **5**). The exchange between the alkoxy ligands is a common step for the three paths described previously and has not been studied in the present work. In the first part, the stable conformers of the postulated intermediates were studied and confirmed as true minima on the potential energy surface. In the second part, the transition states for the postulated steps were located and characterized.

In the calculations, we modeled the diamine ligand by two  $\text{NH}_3$  and the cyclooctadiene (COD) ligand by two ethylene  $\text{C}_2\text{H}_4$  molecules. The carbonyls were modeled by formaldehyde and acetone, and we performed some calculations with acetophenone, which is the experimentally used substrate.

## II. Methodology

The calculations were based on the density functional theory (DFT) at the generalized gradient approximation (GGA) level. They were performed with the Gaussian 94 program.<sup>11</sup> We used the Becke's 1988 functional<sup>12</sup> for exchange and Perdew-Wang's 1991 gradient-corrected functional<sup>13</sup> for correlation. For the Rh atom, we used the relativistic effective core potential of Hay and Wadt with the corresponding double- $\zeta$  basis set.<sup>14</sup> A pseudopotential was also used for C, N, and O atoms.<sup>15</sup> The corresponding valence basis set was of 4-1G type<sup>16</sup> with a d polarization function on N ( $\alpha = 0.80$ ), C ( $\alpha = 0.75$ ), and O ( $\alpha = 0.85$ ). For H atoms, we used the Dunning double- $\zeta$  basis set and added a p polarization function on the hydride ( $\alpha = 1.00$ ).

Geometries of reactants and products were fully optimized without any symmetry constraints. Transition state geometries

(10) Farnetti, E.; Graziani, M. In *Metal promoted selectivity in organic synthesis*; Noels, et al., Eds.; Kluwer Academic Publishers: Dordrecht, 1991; pp 191–205.

(11) Frisch, M. J.; Trucks, G. W.; Schlegel, H. B.; Gill, P. M. W.; Johnson, B. G.; Robb, M. A.; Cheeseman, J. R.; Keith, T. A.; Peterson, G. A.; Montgomery, J. A.; Raghavachari, K.; Al-Laham, M. A.; Zakrzewski, V. G.; Ortiz, J. V.; Foresman, J. B.; Cioslowski, J.; Stephanov, B. B.; Nanayakkara, A.; Challacombe, M.; Peng, C. Y.; Ayala, P. Y.; Chen, W.; Wong, M. W.; Andres, J. L.; Replogle, E. S.; Gomperts, R.; Martin, R. L.; Fox, D. J.; Binkley, J. S.; Defrees, D. J.; Baker, J.; Stewart, J. P.; Head-Gordon, M.; Gonzalez, C.; Pople, J. A. *Gaussian 94 (Revision D.1)*; Gaussian, Inc.: Pittsburgh, PA, 1995.

(12) Becke, A. D. *Phys. Rev. A* **1988**, *38*, 3098.

(13) Perdew, J. P.; Wang, Y. *Phys. Rev. B* **1992**, *45*, 13244.

(14) Hay, P. J.; Wadt, W. R. *J. Chem. Phys.* **1985**, *85*, 299.

(15) Bouteiller, Y.; Mijoule, C.; Nizam, M.; Barthelat, J. C.; Daudey, J. P.; Pelissier, M. *Mol. Phys.* **1988**, *65*, 295.

(16) Bouteiller, Y.; Mijoule, C.; Nizam, M.; Barthelat, J. C.; Daudey, J. P.; Pelissier, M. Private communication.

were found via the quasi-Newton algorithms,<sup>17</sup> QST2 or QST3. All transition states were characterized by determining the number of imaginary frequencies,<sup>18</sup> and a further characterization of the transition states was achieved by calculation of the intrinsic reaction coordinate (IRC)<sup>19</sup> leading to the corresponding energy minima.

### III. Results and Discussion

**A. Intermediates Involved in the Catalytic Mechanism. (a) The ML<sub>5</sub> Hydride Complex 1.** In our previous work,<sup>7</sup> we have investigated the various structures of the d<sup>8</sup> model hydride complex (**1**) supposed to be the starting point of the catalytic cycle. We found that complex **1** is most stable in a trigonal-bipyramidal (TBP) geometry, with two NH<sub>3</sub> and two ethylene ligands.

Even if there is no direct proof for its presence during the cycle, the participation of this hydride as a key intermediate seems reasonable. The existence of this d<sup>8</sup>-monohydride complex finds support in some experimental papers dealing with similar hydrides bound to ruthenium<sup>20,21</sup> and rhodium<sup>22–25</sup> and has been often postulated in theoretical papers.<sup>26,27</sup>

**(b) The ML<sub>4</sub> Hydride Complex 2.** The coordination of a carbonyl on **1** can a priori follow two main routes: one is a “S<sub>N</sub>2-like reaction” with concomitant arrival of the carbonyl and departure of NH<sub>3</sub>. The second is a purely dissociative one, in which one NH<sub>3</sub> dissociates reversibly prior to carbonyl coordination, leading to the ML<sub>4</sub> coordinatively unsaturated complex **2** with 16 electrons. The first path has been tested, and we could not find any transition state, one NH<sub>3</sub> ligand moving away from the coordination sphere of the metal when the carbonyl approaches, due probably to unfavorable electronic and steric effects. This is the reason we have studied the ML<sub>4</sub> complex **2**.

The optimized geometry is square-planar (Figure 3). The Rh–N bond is shorter than in **1** (2.19 vs 2.31 Å), and the Rh–H distance is the same. The trans influence of the hydride is noticed, so the Rh–C distances are nearly the same as in **1** (longer for the axial than for the equatorial ethylene).

**(c) The Carbonyl-Coordinated Complexes 3.** We have used formaldehyde (in the following denoted by index *f*) and acetone (index *a*) as models of carbonyls and also the real experimental carbonyl, acetophenone (index *ap*).

The carbonyl ligands can adopt two fundamental modes of coordination on a transition metal complex: end-on coordination (called  $\eta^1$ ) by a lone pair of the

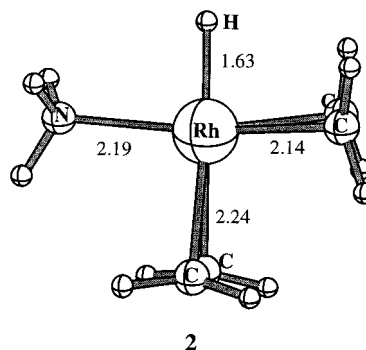


**Figure 3.** Selected geometrical parameters of optimized structures (Å, deg) for the ML<sub>4</sub> hydride complexes **2**.

oxygen atom or side-on coordination (called  $\eta^2$ ) through the CO  $\pi$  system. Because of the axial preference of the hydride shown for **1**,<sup>7</sup> we have excluded the isomers with an equatorial hydride. Starting from different initial structures, we find only one  $\eta^1$ - and one  $\eta^2$ -complex for the formaldehyde and the acetone ligands (presented in Figure 4). For acetophenone, we find two structures with the  $\eta^2$ -coordinated acetophenone (named **3ap- $\eta^2$ -a** and **3ap- $\eta^2$ -b**, Figure 5), because acetophenone is disymmetrically substituted, and one structure with the  $\eta^1$ -coordinated acetophenone (named **3ap- $\eta^1$** , Figure 5); the most stable of the  $\eta^2$ -complexes is the one with the phenyl group opposite H, **3ap- $\eta^2$ -a**. It is energetically favored by 1.1 kcal/mol, which corresponds to a ratio of 88:12 in favor of **3ap- $\eta^2$ -a** at room temperature. It can be noted here that the two complexes **3ap- $\eta^2$ -a** and **3ap- $\eta^2$ -b** would lead to a different enantiomer of 1-phenylethanol after transfer of the hydride.

All the stable structures have a TBP geometry. For the three carbonyls, the favored isomer is  $\eta^2$ -coordinated. The energy difference between the  $\eta^2$  and  $\eta^1$  forms is 15.2 kcal/mol for formaldehyde, 2.1 kcal/mol for acetone, and 2.0 or 3.1 kcal/mol for acetophenone depending on the considered  $\eta^2$  isomer.

A lot of experimental  $\eta^1$ - or  $\eta^2$ -complexes of carbonyls exist depending on the metal and the ligand field. A previous theoretical rationalization has been done with a semiempirical method (EHT).<sup>28</sup> With the present ab initio results, we can confirm these conclusions more quantitatively. Effectively, Scheme 1 shows the relative positions of the frontier orbitals of the ML<sub>4</sub> fragment (obtained by cutting the metal–carbonyl bond) and of the three carbonyls. In the  $\eta^1$  form, the main interaction involves one pair of the oxygen atom, called p(O), and the complex LUMO. In the  $\eta^2$  form, the main interaction involves the vacant  $\pi^*(\text{CO})$  and the HOMO of the metallic fragment. One observes that for formaldehyde the latter interaction is energetically favored over the former one, which leads to a large preference for the  $\eta^2$  form. For acetone, the orbitals are higher than for formaldehyde, the p(O) interaction with the LUMO is increased, and on the contrary, the  $\pi^*(\text{CO})$  interaction with the HOMO is weakened so that the  $\eta^2$  form is only slightly preferred. Acetophenone is an intermediate case between formaldehyde and acetone since the p(O) orbital has roughly the same energy as that of acetone and the  $\pi^*(\text{CO})$  orbital the same energy as that of formaldehyde.

- (17) Peng, C.; Schlegel, H. B. *Isr. J. Chem.* **1993**, 33, 449.  
 (18) Schlegel, H. B. *Theor. Chim. Acta* **1984**, 66, 33.  
 (19) (a) Fukui, K. *Acc. Chem. Res.* **1981**, 14, 363. (b) Gonzales, C.; Schlegel, H. B. *J. Phys. Chem.* **1990**, 94, 5523. (c) Gonzales, C.; Schlegel, H. B. *J. Chem. Phys.* **1991**, 95, 5853.  
 (20) (a) Haack, K.-J.; Hashiguchi, S.; Fujii, A.; Ikariya, T.; Noyori, R. *Angew. Chem., Int. Ed. Engl.* **1997**, 36, 6 (3), 285. (b) Noyori, R.; Hashiguchi, S. *Acc. Chem. Res.* **1997**, 30, 97.  
 (21) Dobson, A.; Robinson, S. D. *Inorg. Chem.* **1977**, 16, 137.  
 (22) La Placa, S. J.; Ibers, J. A. *Acta Crystallogr.* **1965**, 18, 511.  
 (23) Chou, M.; Creutz, C.; Mahajan, D.; Sutin, N.; Zipp, A. P. *Inorg. Chem.* **1982**, 21, 3989.  
 (24) Mahajan, D.; Creutz, C.; Sutin, N. *Inorg. Chem.* **1985**, 24, 2063.  
 (25) Morton, D.; Cole-Hamilton, D. J.; Utuk, D.; Paneque-Sosa, M.; Lopez-Poveda, M. *J. Chem. Soc., Dalton Trans.* **1989**, 489.  
 (26) (a) Koga, N.; Jin, S. Q.; Morokuma, K. *J. Am. Chem. Soc.* **1988**, 110, 3417. (b) Matsubara, T.; Koga, N.; Ding, Y.; Musaev, D. G.; Morokuma, K. *Organometallics* **1997**, 16, 1065.  
 (27) Pidun, U.; Frenking, G. *Chem. Eur. J.* **1998**, 4, 522.

- (28) Delbecq, F.; Sautet, P. *J. Am. Chem. Soc.* **1992**, 114, 2446.



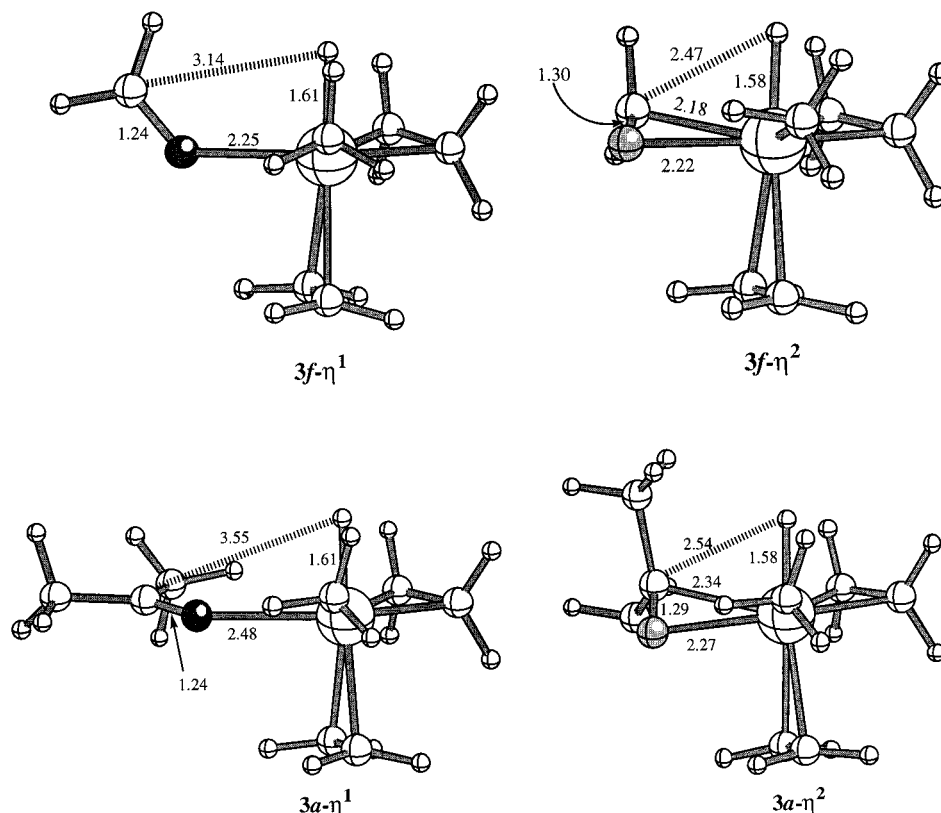
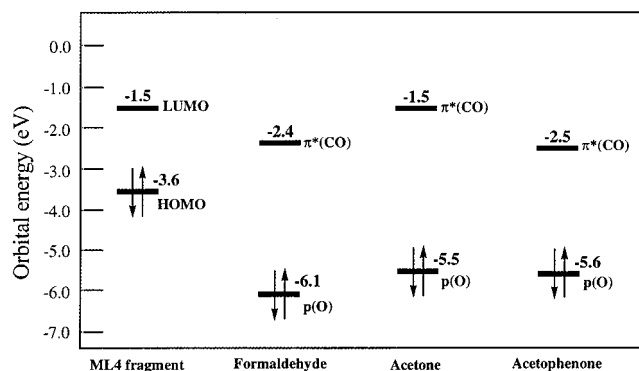


**Figure 4.** Selected geometrical parameters of optimized structures (Å, deg) for  $\eta^1$ - and  $\eta^2$ -complexes **3** of formaldehyde and acetone.

**Scheme 1. HOMO and LUMO Energies of the  $ML_4$  Fragment in Complexes **3** and  $p(O)$  and  $\pi^*(CO)$  Energies for Formaldehyde, Acetone, and Acetophenone**



In the  $\eta^1$ -coordinated complexes of carbonyls (**3f- $\eta^1$** , **3a- $\eta^1$** , and **3ap- $\eta^1$** ), the C–O bond lengths are almost the same as in the free calculated molecules (1.22 Å for formaldehyde, 1.23 Å for acetone, and 1.24 Å for acetophenone). For formaldehyde, the C–O bond is parallel to the Rh–H bond and the distance between this hydrogen atom and the formyl carbon is 3.14 Å. On the contrary, for acetone and acetophenone, the carbonyl plane is the equatorial plane, then the C–O bond is perpendicular to the Rh–H bond and the distance between the migrating hydrogen and the carbonyl carbon atom is longer (3.55 Å in **3a- $\eta^1$**  and 3.38 Å in **3ap- $\eta^1$** ).

In the  $\eta^2$ -coordinated complexes (**3f- $\eta^2$** , **3a- $\eta^2$** , and **3ap- $\eta^2$** ), the carbonyl is in the equatorial plane, as expected for a coordinated double bond.<sup>29</sup> As a conse-

quence of the back-donation into  $\pi^*(CO)$ , the C–O bond lengths are more elongated than in the  $\eta^1$  forms (1.30 Å in the case of formaldehyde and 1.29 Å in the cases of acetone and acetophenone), and a slight rehybridization of the carbon atoms takes place, since the hydrogens bonded to the carbon are tilted outward by 13°. The distances between the hydride and the carbon of carbonyls are 2.47 Å (formaldehyde), 2.54 Å (acetone), and 2.56 Å (acetophenone). Thus the hydride is nearer to the carbonyls in the  $\eta^2$  forms than in the  $\eta^1$  ones, and therefore the  $\eta^2$  forms seem good precursors for hydride migration.

**(d) The  $ML_4$  Alkoxy Complexes **4**.** After the hydride transfer, a  $ML_4$  16-electron complex is obtained with an alkoxy coordinated to the rhodium. Starting from various geometries, in the case of formaldehyde, we obtained two stable methoxy complexes (**4fa** and **4fb**, Figure 6), due to different rotations around the Rh–O bond. Because of an intramolecular hydrogen bond, the **4fa** isomer is the most stable, by 4.1 kcal/mol, and the rotation barrier for the methoxy group around the Rh–O axis is calculated to be 5.6 kcal/mol. This hydrogen bond between one hydrogen of  $NH_3$  and O (distance H–O = 2.04 Å) leads to a small N–Rh–O angle (76° instead of 90° in **4fb**) and a small H–N–Rh angle (96° instead of 112° in **4fb**). Mulliken overlap populations are also consistent with the presence of an interaction between the H of  $NH_3$  and O since for both N–H and Rh–O they are smaller in **4fa** (0.251 and 0.173, respectively) than in **4fb** (0.305 and 0.208, respectively). In addition, a small but positive overlap population, present between H and O in **4fa**, is greatly

(29) Rossi, A. R.; Hoffmann, R. *Inorg. Chem.* **1975**, *14*, 365.

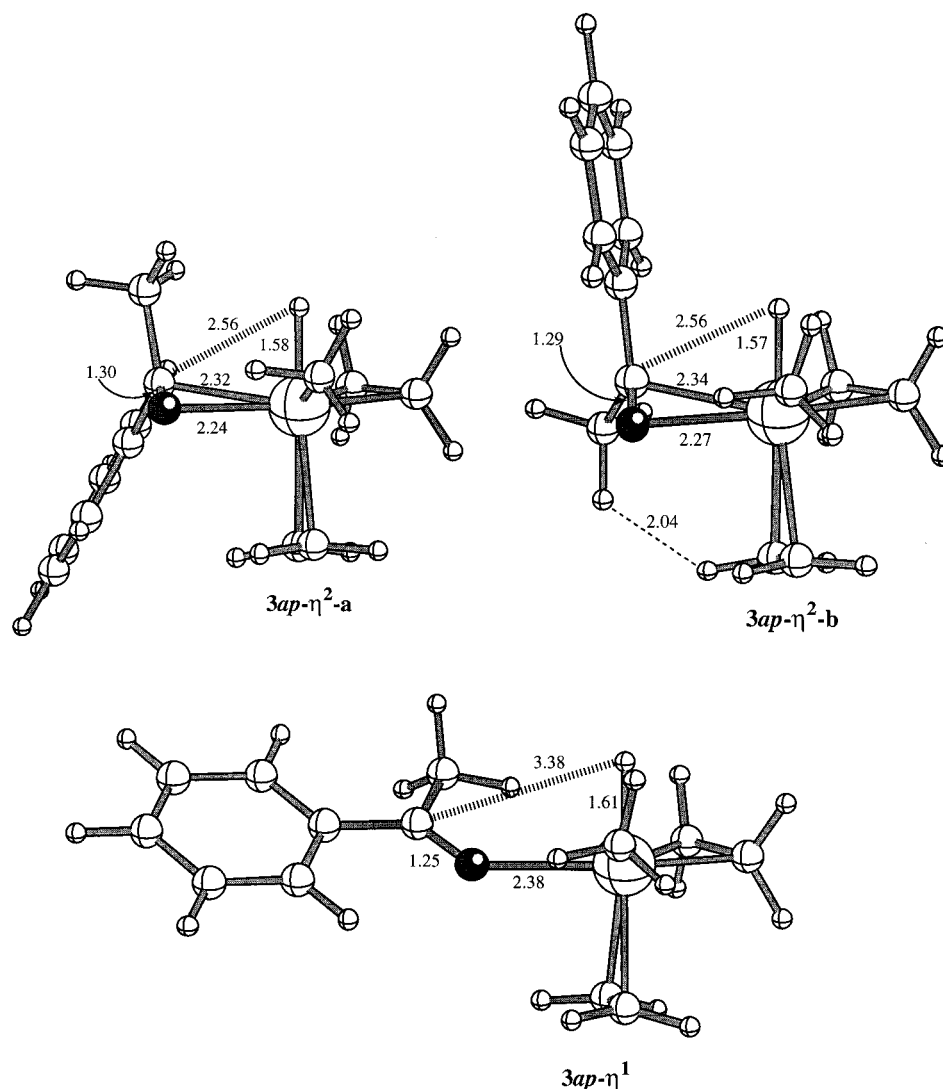


**Figure 5.** Selected geometrical parameters of optimized structures (Å, deg) for the two isomers of the  $\eta^2$ -complex of acetophenone and the  $\eta^1$ -complex of acetophenone.

diminished in **4fb** (0.042 in **4fa** vs 0.003 in **4fb**). In some organometallic complexes, intramolecular interaction between one N–H ligand and the lone pair of an electronegative atom such as nitrogen, oxygen, and halogens is a well-known phenomenon, which has been studied spectroscopically by NMR, IR, and X-ray<sup>30</sup> and calculated by ab initio methods.<sup>31</sup> The capability of alkoxy and phenoxy ligands to exhibit hydrogen bonding has been established both in the solid state and in solution.<sup>32</sup>

With acetone, we obtain four isopropoxy complexes (**4a-a**, **4a-b**, **4a-c**, and **4a-d** Figure 6) due to the rotations around the Rh–O and O–C bonds. The **4a-a**

isomer is the most stable probably because of the intramolecular H-bond and the smaller steric constraint between the ethylene and the methyls. The calculated rotation barriers are 7.7 kcal/mol around the Rh–O axis and 5.1 kcal/mol around the O–C bond. In the case of acetophenone, we have only optimized one of the two enantiomer  $ML_4$  complexes (**4ap**, Figure 7) which corresponds to the most stable isopropoxy complex.

All these  $ML_4$  complexes are perfectly planar, and the bond lengths are almost the same. The trans effect of the alcoholate ligand and of the  $NH_3$  ligand is of similar magnitude so the two ethylenes are at the same distance from rhodium.

**(e) The  $ML_5$  Alkoxy Complexes 5.** After recoordination of a  $NH_3$  ligand, we obtained a  $ML_5$  alkoxy complex with 18 electrons. One  $NH_3$  ligand can be coordinated in equatorial or axial position. Starting from all the possible structures for methoxy and isopropoxy ligands, taking into account the rotations around the Rh–O and O–C bonds, the geometry was relaxed. We found three stable structures for methoxy complexes and five for isopropoxy complexes (Figure 8).

The most stable methoxy complex is **5fa**, where the two  $NH_3$  are in equatorial position. There are two

(30) (a) Bronty, C.; Spinat, P.; Whuler, A. *Acta Crystallogr., Sect. B* **1980**, *36*, 1967. (b) Fryzuk, M. D.; MacNeil, P. A.; Rettig, S. J. *J. Am. Chem. Soc.* **1987**, *109*, 2803. (c) Fryzuk, M. D.; Montgomery, C. D. *Coord. Chem. Rev.* **1989**, *95*, 1. (d) Fryzuk, M. D.; Montgomery, C. D.; Rettig, S. J. *Organometallics* **1991**, *10*, 467, and references therein.

(31) Peris, E.; Lee, J. C.; Rambo, J. R.; Eisenstein, O.; Grabtree, R. H. *J. Am. Chem. Soc.* **1995**, *117*, 3485.

(32) (a) Kogley, S. E.; Schaverien, C.; Fredenberger, J. H.; Bergman, R. G.; Nolan, S. P.; Hoff, C. D. *J. Am. Chem. Soc.* **1987**, *109*, 6563. (b) Kim, Y. J.; Osakado, K.; Takenak, A.; Yamamoto, A. *J. Am. Chem. Soc.* **1990**, *112*, 1096. (c) Osakado, K.; Ohchiro, K.; Yamamoto, A. *Organometallics* **1991**, *10*, 404. (d) Alsters, P. L.; Baesjou, P. J.; Janssen, M. D.; Kooijman, H.; Sicherer-Roetman, A.; Spek, A. L.; Koten, G. *Organometallics* **1992**, *11*, 4124.

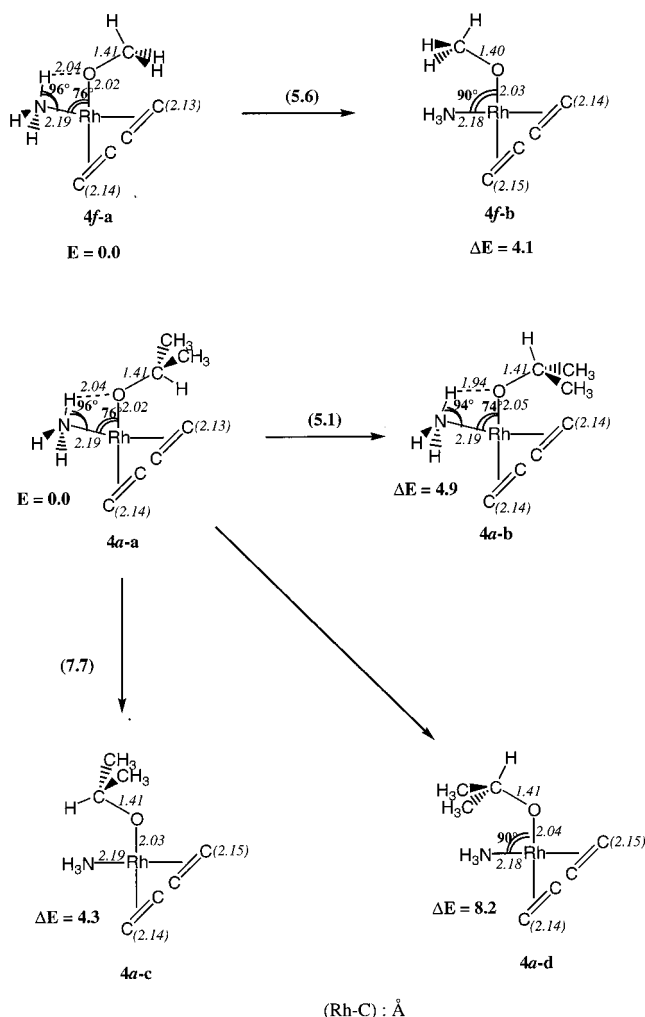


**Figure 6.** Selected geometrical parameters of optimized structures (Å, deg) for the isomers of the ML<sub>4</sub> methoxy and isopropoxy complexes **4** and the energies (kcal/mol) relative to **4f-a** and **4a-a**. In parentheses, rotation barriers around the Rh–O and O–C axis.

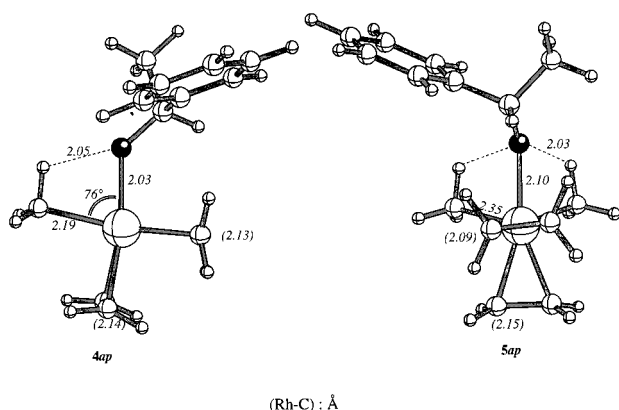


**Figure 7.** Selected geometrical parameters of optimized structures (Å, deg) for ML<sub>4</sub> and ML<sub>5</sub> acetophenoxy complexes.

hydrogen bonds between the hydrogens of the NH<sub>3</sub> ligands and the oxygen of the alkoxy ligand (distance between H and O is 2.02 Å), so the angles N–Rh–O and H–N–Rh are relatively small, 75° and 89°, respectively. This complex is more stable than **5f-b** (with NH<sub>3</sub> in axial position) by 3.3 kcal/mol and than **5f-c** by 3.9 kcal/mol.

The most stable isopropoxy complex is **5a-a**. Like the methoxy complex, it has the two NH<sub>3</sub> ligands in equatorial position and two hydrogen bonds between the hydrogens of the NH<sub>3</sub> groups and the oxygen of the alkoxy group (distance between H and O is 2.02 Å). The angles N–Rh–O and H–N–Rh are also relatively small, 74° and 89°, respectively. The other bond lengths are the same as in **5f-a**.

In the case of acetophenone, we have optimized only one of the two enantiomer ML<sub>5</sub> complexes (**5ap**, Figure 7) which correspond to the most stable isopropoxy complex. A similar geometry is obtained.

In the most stable ML<sub>5</sub> alkoxy complexes, the geometry resembles that of the hydride ML<sub>5</sub> complex **1**. One can remark, however, that the trans effect of the alkoxy group is smaller than that of the hydride (distances between Rh and the axial carbons are around 2.20 Å in **1** and 2.15 Å in **5a-a**).

**B. Elementary Reaction Steps and Their Transition States.** Up to now we have shown that all the postulated intermediates in the catalytic cycle exist and are minima on the potential energy surface. Even if for each intermediate there are several isomers, in most cases, one is clearly more stable. Of course, the mechanism depends heavily on the activation energies of the individual reaction steps, which will be discussed in this section, together with the transition states between each most stable intermediate.

The reaction cycle of carbonyl reduction, as seen in Figure 2, involves nine elementary reaction steps: (i) dissociation of N-ligand, (ii) carbonyl addition, (iii) hydride migration, (iv) recoordination of N-ligand, (v) exchange of alcoholate ligands, (vi) decooordination of N-ligand, (vii) β-H transfer, (viii) carbonyl elimination, and (ix) N-ligand recoordination; the last four elementary reactions are the reverse of the first four ones, so we only have to investigate half of the cycle.

**(a) Nitrogen Ligand Decoordination: TS(NH<sub>3</sub>) and TS(NH<sub>2</sub>–CH<sub>2</sub>–CH<sub>2</sub>–NH<sub>2</sub>).** From the starting model hydride complex, we have to decoordinate reversibly a ligand, to allow for the coordination of a carbonyl. Dissociation energies of NH<sub>3</sub> ligands and ethylene ligands have been studied,<sup>7</sup> and according to the difference (4 kcal/mol for NH<sub>3</sub> compared to 18 or 21 kcal/mol depending on the position of the leaving ethylene), NH<sub>3</sub> is more easily decoordinated than ethylene. Hence, we have tried to find the transition state for decooordination of different nitrogen ligands.

First, we have studied the dissociation of the simplest N-attached ligand, NH<sub>3</sub>, from **1** to **2** (TS(NH<sub>3</sub>) in Figure 9). We have found a transition state 2.8 kcal/mol higher than **1**. Following the eigenvector corresponding to the negative eigenvalue of the Hessian (IRC calculations<sup>18</sup>), we found the hydride complex **1**. In the opposite direction, we did not obtain the isolated molecules (**2** and NH<sub>3</sub>) but a complex stabilized by a hydrogen bond between the nitrogen of the decoordinated NH<sub>3</sub> and a hydrogen of the NH<sub>3</sub> moiety. This complex is 8.8 kcal/mol more stable than the two isolated fragments, and the reaction is exothermic by 4.5 kcal/mol. The transition state has the leaving NH<sub>3</sub> in the equatorial plane, at 2.71 Å from the metal, and the hydrogen bond is not yet formed (the N–H distance is 2.58 Å). The distance between the metal and the coordinated NH<sub>3</sub> is shorter

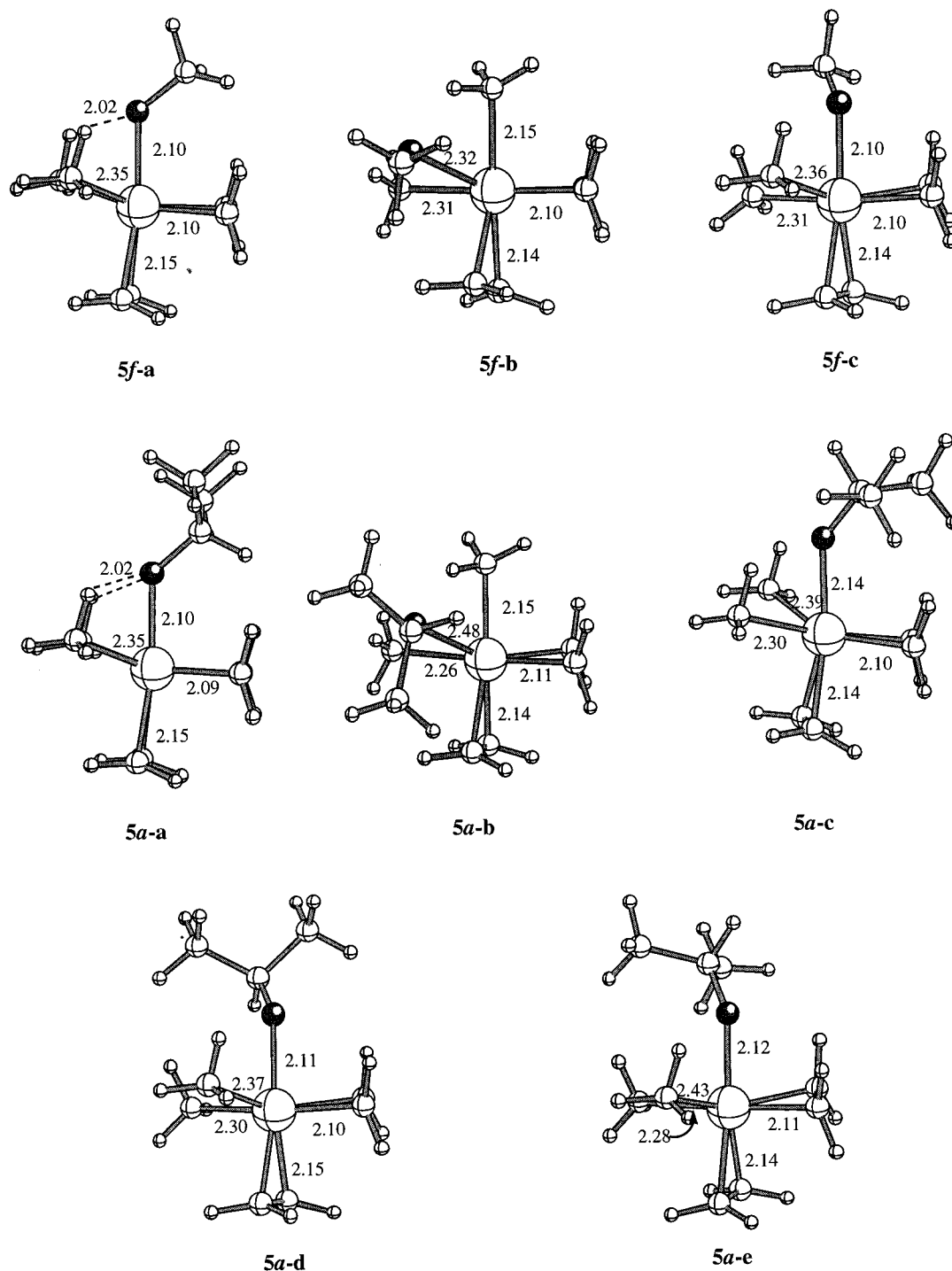


**Figure 8.** Selected geometrical parameters of optimized structures (Å, deg) for the isomers of the  $ML_5$  methoxy and isopropoxy complexes **5**.

than in **1** (2.25 vs 2.32 Å), and this ligand begins to move toward the trans position with respect to the equatorial ethylene.

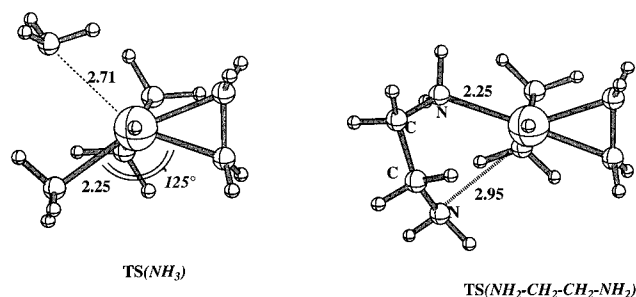
To study the difference between  $NH_3$  ligands and a more realistic bidentate ligand (the diamine:  $NH_2-CH_2-CH_2-NH_2$ ), we have tried to locate the transition state for breaking a  $Rh-N$  bond of the diamine complex. We have employed the reaction coordinate method followed by a transition state search based on the Berny algorithm.<sup>33</sup> The activation barrier for this decooordination has been found to be 7.7 kcal/mol, and the reaction is endothermic, but only by 1.4 kcal/mol. The geometry of the transition state (**TS**( $NH_2-CH_2-CH_2-NH_2$ ) in

Figure 9) is almost square-planar, showing that it is a rather product-like transition state. To our knowledge, such a transition state for decooordination of a bidentate ligand has never been investigated. The small activation barrier shows that with a diamine ligand the decooordination is also possible.

**(b) Coordination of Carbonyls.**  $\eta^2$ -Coordination of formaldehyde to the unsaturated complex **2** is exothermic by 15.1 kcal/mol. Addition of acetone in the  $\eta^2$  form to **2** is almost thermoneutral ( $\Delta E = -0.2$  kcal/mol), and addition of acetophenone in the  $\eta^2$  form to **2** is weakly

(33) Schlegel, H. B. *J. Comput. Chem.* **1982**, 3, 214.





**Figure 9.** Optimized geometries (Å, deg) for the transition states for the NH<sub>3</sub> decoordination, **TS(NH<sub>3</sub>)**, and for the breaking of a Rh–N bond with the diamine ligand, **TS(NH<sub>2</sub>-CH<sub>2</sub>-CH<sub>2</sub>-NH<sub>2</sub>)**.

**Table 1.** Energies of  $\eta^2$ -Complexes **3**, Transition States for the Hydride Migration, **TS(3→4)**, and ML<sub>4</sub> Alkoxy Complexes **4**<sup>a</sup>

structures	$\Delta E$ (kcal/mol)
<b>Formaldehyde</b>	
<b>3f-<math>\eta^2</math></b>	0.0
<b>TS(3f-<math>\eta^2</math>→4fa)</b>	8.9
<b>4fa</b>	-16.2
<b>Acetone</b>	
<b>3a-<math>\eta^2</math></b>	0.0
<b>TS(3a-<math>\eta^2</math>→4a-a)</b>	6.8
<b>4a-a</b>	-16.8
<b>Acetophenone</b>	
<b>3ap-<math>\eta^2</math>-a</b>	0.0
<b>TS(3ap-<math>\eta^2</math>-a→4ap-a)</b>	8.4
<b>4ap-a</b>	-14.5
<b>3ap-<math>\eta^2</math>-b</b>	1.1 (0.0)
<b>TS(3ap-<math>\eta^2</math>-b→4ap-b)</b>	8.4 (7.3)
<b>4ap-b</b>	-14.5 (-15.6)

<sup>a</sup> For formaldehyde, energies are relative to **3f- $\eta^2$** ; for acetone, energies are relative to **3a- $\eta^2$** ; for acetophenone, the energies are relative to **3ap- $\eta^2$ -a**, and in parentheses, energies are relative to **3ap- $\eta^2$ -b**.

exothermic ( $\Delta E = -3.6$  or  $-2.5$  kcal/mol depending on the coordinated face).

While this work was in progress, it was reported<sup>26</sup> that a possible mechanistic prototype for the addition of carbonyls to a coordinatively unsaturated transition metal complex is as follows: first, the formation of an end-on complex (due to the fact that at large distances the electrophilic metal starts to interact with the free electrons of the carbonyl oxygen atom) and, second, the rearrangement to the most stable side-on complex. In our case, one can suppose the same path.

Despite an extensive search, no transition state connecting the reactants, "**2** + carbonyl", and the product could be found, indicating that the carbonyl coordination reaction takes place without a barrier.

**(c) Hydride Migration: TS(3→4).** Starting from the  $\eta^2$ -coordinated complexes **3**, we have investigated the hydride migration step leading to the alkoxy complexes **4**. For each carbonyl, we have located a transition state. In Table 1 are collected the energetic results for the three carbonyls. One observes that the reactions are exothermic (by 14–17 kcal/mol) and that the activation barriers are relatively low (6–9 kcal/mol). So, in this direction the activation barriers are not too high and the hydride migration can take place at room temperature.

With acetophenone, two transition states are possible, depending on the position of the phenyl substituent. The

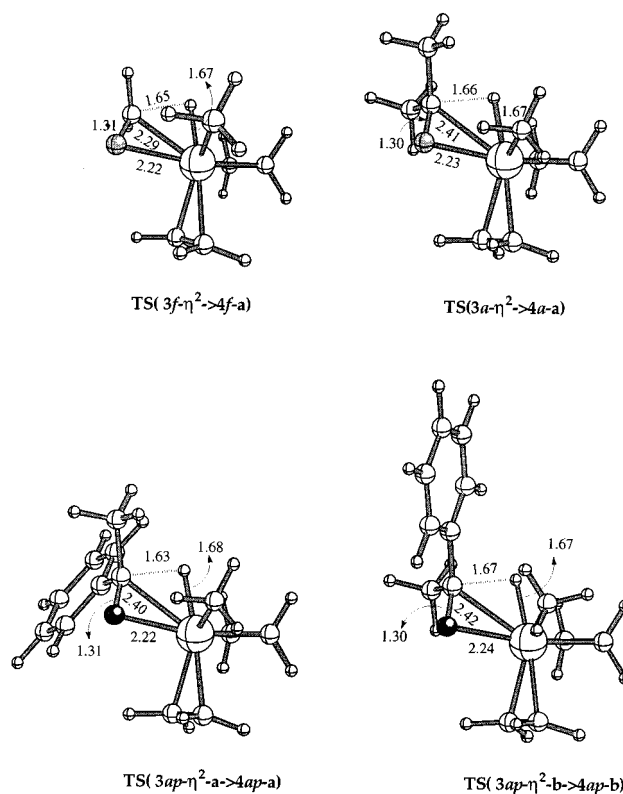


**Figure 10.** Optimized molecular geometries (Å, deg) of the transition states **TS(3→4)** (which connects intermediates **3** and **4**), in the case of formaldehyde, acetone, and acetophenone.

two transition states have the same energy, indicating that the interactions between substituents of the carbonyls and the ligands of rhodium are in this case not important. A difference between these two transition states could however arise in the case where larger substituents are used on the amine ligand. Despite the similar energies for the transition states, the activation energies for the hydride migration are not the same, because of the different stability of the  $\eta^2$  forms. The less stable (hence the minor)  $\eta^2$ -complex (see section A-(c)) leads to the alkoxy complex **4** with the smallest activation barrier (7.3 vs 8.4 kcal/mol), which corresponds to a reaction about 10 times faster. Hence it is kinetically favored. But if one considers the energetics of the cycle (Figure 11) and the activation barriers, one observes that the first step (decoordination of NH<sub>3</sub> and coordination of the acetophenone) is reversible. Hence an equilibrium between **3ap- $\eta^2$ -a** and **3ap- $\eta^2$ -b** via the complex **1** is possible. So, the less stable complex, **3ap- $\eta^2$ -b**, is consumed faster, and therefore, this is mainly **3ap- $\eta^2$ -a**, which goes back to **1**. This leads to an enhancement in the production of **3ap- $\eta^2$ -b** and therefore to a racemization after the hydride transfer. In other words, the effective barriers to form the two enantiomers **4ap** from the reactants (**1** + acetophenone) are quasi identical. Therefore, as could be expected from experimental results,<sup>3</sup> such a reaction mechanism yields no enantioselectivity if model nonchiral amine ligands are considered.

The transition states are presented in Figure 10. They are early: the Rh–C bond, which is the bond being broken, is less than 5% longer than in the  $\eta^2$ -complex. The hydrogen is only 6% farther from Rh (1.67 vs



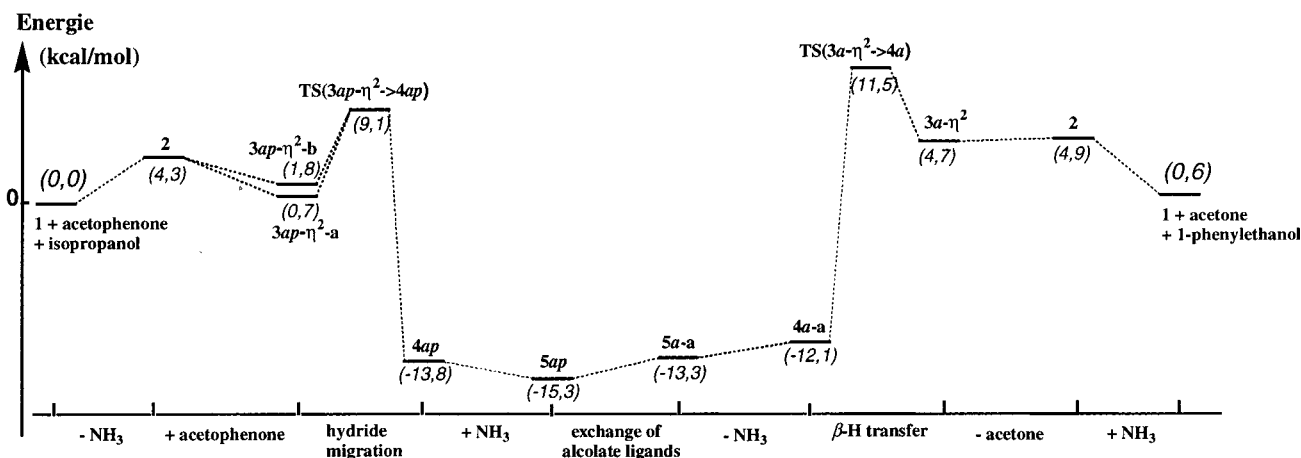


**Figure 11.** Calculated reaction profile (kcal/mol) of the entire catalytic cycle for the hydride transfer between acetophenone and 2-propanol catalyzed by **1**. Only the most stable isomers are considered. All the energies reported refer to the reference state "1 + acetophenone + 2-propanol". See text for details.

1.58 Å in the  $\eta^2$ -coordinated complex), and the Rh–O bond is only a little shorter (2%). The C=O bond has rotated around Rh–O and is parallel to the Rh–H bond, making a four-center transition state with a C–H bond elongated to 1.65 Å. During the hydrogen migration, the equatorial  $\text{NH}_3$  ligand moves to the vacant coordination site that H left to generate a  $\text{ML}_4$  alkoxy complex **4**.

As mentioned in a previous section, several isomers exist for product **4**, and in our search for the transition state, we have supposed that the final product was the most stable  $\text{ML}_4$  alkoxy (**4fa** for formaldehyde, **4a-a** for acetone, and **4ap** for acetophenone). This was confirmed by IRC calculations.<sup>18</sup>

**(d) Reoordination of Nitrogen Ligands.** With the three studied carbonyls, the reoordination of a  $\text{NH}_3$  ligand to give the most stable  $\text{ML}_5$  alkoxy complex is an exothermic process (by 1.7 kcal/mol for formaldehyde, by 1.2 kcal/mol for acetone, and by 1.5 kcal/mol for acetophenone).

We have not studied the kinetic aspect of this step, but since the starting complex is the same as in section **B(a)** (the difference is the substitution of the hydride ligand by an alkoxy ligand), one can think that it is almost the reverse reaction of coordination of nitrogen ligand to complex **1**. So we can suppose that the activation barrier is almost the same (7.3 kcal/mol for  $\text{NH}_3$  and 6.3 kcal/mol for the diamine).

As said before, we have not focused on the mechanism of exchange of alkoxy ligands. However, the exchange between 2-propanol and phenylethanol is thermodynamically in favor of **5ap** by 2 kcal/mol.

**(e) Catalytic Cycle.** Figure 11 shows the calculated energy profile for the entire catalytic cycle, with  $\text{NH}_3$  and ethylene ligands and with acetophenone as substrate. Only the activation barriers of the hydride migration on the  $\eta^2$ -complex of acetophenone and the  $\beta$ -H transfer from the  $\text{ML}_4$  isopropoxy complex are shown, because they are found to be the rate-limiting ones. In this profile, the additional molecules (acetophenone and 2-propanol) are considered at infinite distance. The energy difference between the final state (**1** + acetone + 1-phenylethanol) and the initial state (**1** + acetophenone + 2-propanol) of the cycle is the energy of reduction

of acetophenone and of oxidation of 2-propanol. This reaction is weakly endothermic by 0.6 kcal/mol.

The second part of the cycle, leading again to **1**, involves four elementary reactions (decoordination of N-ligand,  $\beta$ -H transfer, carbonyl elimination, and N-ligand reoordination), which are the reverse of the four ones already described. The  $\beta$ -H transfer (from **4** to **3**) to form the acetone has the most important activation barrier (23.6 kcal/mol), which is nevertheless reasonable, and the cycle can be terminated.

The energy profile is quasi symmetrical without too high an activation barrier. So the catalytic cycle can be reversible at room temperature, which has also been postulated experimentally.<sup>3,8</sup>

The energetics of the reaction is almost thermoneutral, and the driving force to favor the formation of the 1-phenylethanol is the excess of 2-propanol (the solvent), which displaces the equilibrium.

#### IV. Conclusion

In the present work, we studied, with the help of DFT calculations, one of the possible mechanisms (the two-step mechanism) for the reduction of carbonyls catalyzed by a rhodium(I) hydride complex. On the basis of our calculations, we showed that all the postulated intermediates are minima on the potential energy surface. For each intermediate there are several isomers, and in most cases, one is clearly the most stable. The thermodynamic profile of the full cycle is found to be smooth, without excessive barriers, the overall reactions being quasi thermoneutral. The first step corresponds to the dissociation of a N–Rh bond, yielding the decoordination of one ammine group. This step is weakly endothermic for the realistic diamine ligand with a low activation energy. The following coordination of the carbonyl is then downhill by 0.2–15 kcal/mol depending on the chosen carbonyl. The crucial step of the reaction is then the hydride migration, together with the "reverse"  $\beta$ -H transfer in the second part of the cycle. The hydride transfer has a low activation barrier (6–9 kcal/mol depending on the coordinated carbonyl), but this reaction is significantly exothermic (by 14–17 kcal/mol). As a result, the "reverse"  $\beta$ -H transfer step in the cycle

is associated with a higher barrier of 23 kcal/mol. This step is the rate-limiting one, but the barrier remains reasonable.

Even if the two isomer  $\eta^2$ -complexes of acetophenone have a different energy, this cannot explain, with these model complexes, the observed enantioselectivity since the transition states for hydride migration have the same energy. The discrimination is not an intrinsic property of the complex but is, as expected, due to the chiral ligands. The key and future step is to investigate whether, from this mechanism and with the real chiral diamines, the experimental selectivity can be explained.

The concerted mechanism proposed by Gladiali<sup>5</sup> is presently under investigation. This mechanism has sim-

ilarities to the one recently supposed by Noyori.<sup>20</sup> This author reported the enantioselective reduction of ketones from 2-propanol, using a Ru(II) complex and bidentate ligands.

**Acknowledgment.** The authors thank IDRIS (Institut du Développement et des Ressources en Informatique Scientifique du CNRS) and the Pôle Scientifique de Modélisation Numérique at ENS-Lyon for their computational support.

OM990603N